

Molecular modeling of voltage-gated potassium channel pore

ZHAO Shan-Rong, CHEN Kai-Xian¹, WANG Wei, GU Jian-De, HU Zeng-Jian, JI Ru-Yun
(Shanghai Institute of Materia Medica, Chinese Academy of Sciences, Shanghai 200031, China)

KEY WORDS molecular models; potassium channels; protein conformation; ion transport; computer-aided design

AIM: To build a structure model for the pore of voltage-gated *Shaker* potassium channel and examine its validity. **METHODS:** (1) Structural restraints were derived from experimental and theoretical studies; (2) An initial structural motif satisfying the derived restraints was first constructed, and further refined by restrained molecular mechanics; (3) The quality of the model was judged by the criterion that whether it could clarify molecular mechanisms of channel functions and explain the known experimental facts.

RESULTS: (1) A computer pore structure was proposed, in which the residues within signature sequence (corresponding to *Shaker* 439-446) dipped into the membrane and formed the narrow part of the pore in a non-periodic conformation, while the other residues in the P region constituted the outer mouth of the pore; (2) The ion selectivity was achieved through cation- π orbital interaction mechanism at position 445 and oxygen cage mechanism at position 447; (3) Different binding modes led to different affinity of CTX and AgTx2 to channel; and (4) The inside of pore was dominated by negative electrostatic potential. **CONCLUSION:** The model proposed was consistent with the derived restraints from the experimental results.

Voltage-gated K⁺ channels were tetrameric integral membrane proteins and responsible for the propagation and transduction of cellular signals.

¹Correspondence to Prof CHEN Kai-Xian. Phn: 86-21-6431-1833. Fax: 86-21-6437-0269. E-mail: kxchen@ims3.shnm.ac.cn
Abbreviations: AgTx2, agitoxin 2; CTX, charybdotoxin; KTX, kalitoxin; MTSEA, methanethiosulfonate-ethylammonium; MTSES, methanethiosulfonate-ethylsulfonate; MTSET, methanethiosulfonate-ethyltrimethylammonium; MTSX, collectively refers to MTSEA, MTSET, MTSES; NMR, nucleic magnetic resonance; SCAM, substituted cysteine accessibility method.

Received 1996-10-30

Accepted 1997-01-29

Each of the subunit consisted of 6 hydrophobic membrane-spanning segments S1-S6. Mutagenesis study had identified that the P region also called H5, SS1-SS2) between hydrophobic domains S5 and S6 contributed substantially to the formation of the pore. Mutations in this region greatly affected the channel properties, eg, ion selectivity, conductance, sensitivity to channel blockers.

Due to combined application of recombinant DNA manipulation of channel sequences and high resolution electrophysical analysis, many structural features of the pore were revealed recently, such as the orientation of side chains and distance restraints among residues in the P region. Unfortunately, there was no structural information directly available from X-ray or NMR to date, mainly because of the difficulty of isolation and crystallization of membrane protein.

To shed light on the molecular mechanism of channel function, a helical hairpin motif was proposed in 1995, in which 2 α -helices were connected by a short loop, with the loop carbonyl oxygens responsible for ion selectivity^[1]. Another structural motif was also constructed with only the residues on the C-end of pore region lining directly to the inner wall of pore^[2]. These 2 models agreed well to many known facts, but could not explain explicitly the mutation results on the N-end residues.

The aim of this work was to propose a more rational computer model for the pore based upon the latest known experimental and theoretical results, so as to enhance our understanding the molecular mechanism of channel functions and guide further studies on potassium channel.

MATERIALS AND METHODS

The *Shaker* pore sequence was defined as the following stretch of amino acids:

425:FFKSIPDAFWAVVTMTTVGYGDMIP:450

The numbering referred to the sequence of 600 amino acids that made up a complete a subunit of *Shaker* K⁺

channel.

Reasoning and derivation of structural restraints The crude topological arrangement of residues in the P region could be elucidated and located by multiple sequence alignment⁽³⁾, together with results from site-directed mutagenesis. The conserved residues tended to be buried in the membrane and/or functionally important, while those residues important for scorpion toxin affinity were likely to line the extracellular entry of the channel, since toxin blocked K⁺ channels with 1:1 stoichiometry and covered the K⁺ conduction pathway by binding to a receptor located near its opening to external solution.

SCAM was widely employed to determine the side-chain orientations of residues in the pore⁽⁴⁻⁷⁾. After each individual residue was mutated to cysteine, the side-chain projection could be detected by assessing the sensitivity of the mutated channel to thiol-labeling reagents (Ag⁺ or MTSX). If its side chain projected to the inside of the pore, the resulting channel reacted with these sulfhydryl-specific reagents, and the channel ion selectivity and conductance changed accordingly.

The relative distances between residues in the pore-forming region were inferred from the structures of molecular probes such as CTX, AgTx2, and KTX. Since these toxins

blocked K⁺ channel pores by binding specifically to a receptor site located at the external vestibule of the channels, the identification of specific pairs of interacting partners in the toxin-channel bound complex led to a picture of the spatial locations of residues on the structurally unknown channels⁽⁸⁻¹²⁾.

Strategies and procedures for modeling The modeling was performed on Silicon Graphics Indigo XZ4000 workstations using InsightII graphics environment developed by Biosym Technologies (Tab 1).

The initial conformations for residues 425-438 and 445-449 were designated according to the derived characteristic of secondary structures. The primary model was further optimized by restrained molecular mechanics using Discover 3 module of InsightII. The aim of optimization was to adjust the shape and dimension of the outer mouth of the pore so as to satisfy those restraints obtained. During the minimization, the backbone of the α -helix was kept fixed, and many distance restraints were applied (Tab 2).

Validation and assessment of model The quality of the model was judged by the criterion that whether it could clarify molecular mechanisms for channel function and explain the known experimental facts.

Tab 1. Procedures for constructing pore initial model.

Construct initial templates:					
P1	431-438:	α -helix;	425-430:	extended conformation	
P2	445-449:	β -strand			
Define alternative axes:					
		P1		P2	
	Original point:	431 C β atom		447 C α atom	
	X direction atom:	438 C β atom		449 C α atom	
	Y plane atom:	mass centroid of 434, 435 C β atoms		447 backbone carbonyl oxygen	
Overlap the two alternative axes of P1 and P2					
Copy the template P1 to P1A, P1B, P1C, P1D; P2 to P2A, P2B, P2C, P2D					
		P1A	P1B	P1C	P1D
	Rotate along X axis degree	0.0	90.0	180.0	270.0
	Shift along the positive Y-direction ¹ nm	0.7	0.7	0.7	0.7
	Rotate along Z axis ² degree	-53.0	-53.0	-53.0	-53.0
		P2A	P2B	P2C	P2D
	Rotat along X axis ³ degree	45.0	135.0	225.0	315.0
	Shift along the positive Y-direction nm	0.7	0.7	0.7	0.7
Merge P1A, P1B, P1C, P1D, P2A, P2B, P2C, P2D					
Generate the conformation of residues 439-444 by loop search in Biosym/Homology module					

¹ Adjust the relative position of different segments; ² tilt the α -helix so as to position residues 431 and 438; ³ fix the relative position of subregions P1 and P2.

Tab 2. Distance restraints used for optimization. X denotes the mass centroid of the corresponding residue's side chain; The 4 subunits are designated as A, B, C, D in turn, among which subunit A is opposite to subunit C. Because of the pore symmetry, we do not list the corresponding information between subunit B and subunit D.

Atom pairs		Initial nm	Restrains		Final nm
Atom 1	Atom 2		Constant K	Distance nm	
A:425:X	C:425:X	6.95	10.0	3.20	3.21
A:427:X	C:427:X	5.52	10.0	3.30	3.27
A:429:X	C:429:X	4.06	10.0	3.40	3.40
A:445:C _α	C:425:C _α	1.32	10.0	0.0 (relative)	1.39
A:445:C _β	C:425:C _β	1.12	100.0	0.0 (relative)	1.09
A:447:C _α	C:427:C _α	1.40	10.0	1.31	1.34
A:447:C _β	C:427:C _β	1.43	100.0	1.14	1.14
A:448:C _α	C:448:C _α	1.29	10.0	1.25	1.22
A:448:C _β	C:448:C _β	1.38	100.0	1.18	1.22
A:449:X	C:449:X	1.43	100.0	1.10	1.10

Docking scorpion toxins CTX and AgTx2 into the vestibule of the channel was carried out using Dock/InsightII module (Biosym Technologies). After that, the binding differences between CTX and AgTx2 was examined by comparing the two resultant complexes. The electrostatic potential of the pore was calculated by Delphi/InsightII module (Biosym Technologies). In order to display the results calculated by Delphi more clearly, the values of electrostatic potential were mapped onto five discrete planes cross-sectioning the channel pore.

RESULTS AND DISCUSSION

Modeling of K⁺ channel pore A complete sequence alignment revealed that all the K⁺ channels were highly homologous over a stretch of 8 amino residues corresponding to the sequence TMTTVGYG in the *Shaker* voltage-activated K⁺ channel (Tab 3).

This homologous region, which we referred to as the signature sequence, probably dipped into the membrane plane in a nonperiodic conformation from the extracellular surface and formed the selectivity filter of pore. Accordingly, the rest of the P region constituted the outer mouth of the pore. This structural inference was favored by the fact that mutations in this region had a diverse effect on

channel ion selectivity^[15]. It was also supported by the finding that mutations of numerous residues outside the signature sequence altered CTX affinity dramatically^[8].

The SCAM results of *Shaker* channel were somewhat different from that of Kv2.1 at certain positions due to different experimental materials and methods (Tab 4). Residues F425, K427, D431, W434, W435, V438, V443, Y445, D447, M448, T449 projected their side chains into the pore lumen based upon the SCAM results of *Shaker* K⁺ channel while referring to other information (Fig 1).



Fig 1. Orientations and secondary structure of residues in the P region.

From the characteristics of the side-chain orientations, we could easily gain insight into the secondary structure motif of the P region. It was obvious that the exposure pattern of residues 431 - 438 was consistent with the α-helical periodicity (Fig 1), and that the 3 consecutive residues 447, 448, and 449 were in a non-periodic conformation.

The known scorpion toxins consisted of 37 - 39 amino acids, including 6 cysteine residues. Detailed NMR structures of CTX, AgTx2, and KTX showed nearly identical polypeptide backbones maintained rigidly by 3 disulfide bonds. The entire internal space of these peptides was filled by those 6 cysteine residues, whereas all non-cysteine residues were surface-exposed and projected into aqueous solution. These structural characteristics made CTX and AgTx2 particularly well suited to analyze the roles of individual residues in the toxin-receptor interaction surface. They favored the likelihood that point mutants would exert only local effects on toxin binding. This locality of point mutations underlay the utility of these toxins as structural probes of the channels. Hence, the derived distance restraints between residues in the P region probed by these toxins were very reliable and reasonable (Tab 5).

These derived physical features for *Shaker* K⁺ channel were depicted in Fig 2. The narrow K⁺

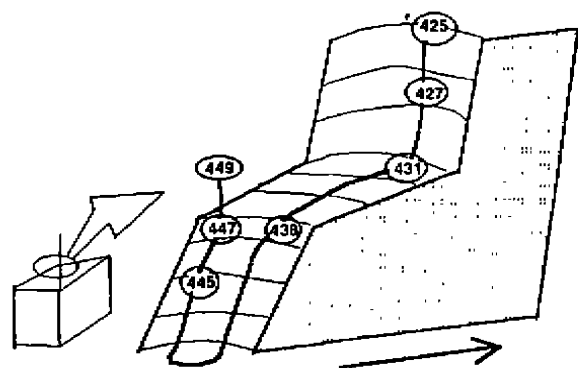
Tab 3. Sequence alignment of P region from different cloned K⁺ channels. The “-” denotes identity with the topmost *Shaker* sequence, while “=” denotes a conservative substitution. The consensus sequences for either the Kv family alone (below rKv6.1), or all K⁺ consensus (bottom), represent positions that either are completely conserved (upper case) or at which a single amino acid predominates (lower case).

Species	Sequence										Kv consensus																				
	425	431	438			445	450																								
<i>Shaker</i>	F	F	K	S	I	P	D	A	F	W	W	A	V	V	T	M	T	T	V	G	Y	G	D	M	T	P					
rK1(RCK1)	H	-	S	-	-	-	-	-	-	-	-	-	-	=	-	-	-	-	-	-	-	-	-	-	-	Y	-				
Shab	K	-	V	-	-	-	=	-	-	-	-	-	G	=	-	-	-	-	-	-	-	-	-	-	-	=	C	-			
rKv2.1(DRK1)	K	-	-	-	-	-	A	S	-	-	-	-	T	=	-	-	-	-	-	-	-	-	-	-	-	=	Y	-			
Shaw	D	-	N	-	-	-	L	G	L	-	-	-	=	-	-	-	-	-	-	-	-	-	-	-	-	-	-	A	-		
rKv3.1(KV4)	H	-	-	N	-	-	I	G	-	-	-	-	-	-	-	-	-	-	-	=	-	-	-	-	-	-	-	Y	-		
Shal	K	-	T	-	-	-	A	-	-	-	-	=	T	=	-	-	-	-	-	=	-	-	-	-	-	-	-	V	-		
mKv4.1(mShal)	N	-	T	-	-	-	A	-	-	-	-	=	T	=	-	-	-	-	-	=	-	-	-	-	-	-	-	V	-		
rKv5.1(IK8)	L	-	-	-	-	-	Q	S	-	-	-	-	=	=	-	-	-	-	-	-	-	-	-	-	-	-	=	Y	-		
rKv6.1(KI3)	E	-	T	-	-	-	A	C	-	-	-	-	=	-	-	-	-	-	-	-	-	-	-	-	-	-	-	V	-		
	F	s	I	P			f	W	w	a		v	t	M	T	T	v	G	Y	G	D	m	P								
ECOKCH	R	I	E	-	=	M	T	-	-	=	=	S	=	E	-	-	=	-	-	-	-	-	-	=	V	-					
Slo	H	R	L	-	Y	W	T	C	V	=	=	L	=	-	-	-	=	-	-	-	-	-	-	=	Y	C					
mSlo	Q	A	L	-	Y	W	=	C	V	=	L	L	=	-	-	-	=	-	-	-	-	-	-	=	Y	A					
KAT1	L	=	N	R	Y	V	T	-	L	=	-	S	=	T	-	=	-	-	T	-	-	-	-	-	F	H	A				
AKT1	L	=	N	R	Y	V	T	S	M	=	-	S	=	T	-	=	-	-	T	-	-	-	-	-	=	H					
ROMK1	N	I	N	G	=	T	S	-	-	L	=	S	=	E	-	Q	V	-	=	-	-	-	-	-	F	R	F	V			
IRK1	E	V	N	-	F	T	A	-	-	L	=	S	=	E	-	Q	-	-	=	-	-	-	-	-	F	R	C	V			
GIRK1	N	V	Y	N	F	-	S	-	-	L	=	F	=	E	-	E	A	-	=	-	-	-	-	-	Y	R	Y	I			

Tab 5. Spatial locations of some residues in the pore. The number in parentheses correspond to residue in *Shaker* channel.

Groups	Interacting pairs		Distance away from the pore axis nm
	Toxin	<i>Shaker</i>	
Goldstein <i>et al</i> ^[8]	T8, T9/CTX	F425	425: 1.3–1.5
Stocker and Miller ^[10]	K11/CTX	K427	427: 2.0
Naranjo and MacKinnon ^[11]	M29/CTX	T449	449: about 0.5
Hidalgo and MacKinnon ^[12]	R24/AgTx2	D431	431: 1.2–1.5
Ajar <i>et al</i> ^[9]	R24/KTX	D386/Kv1.3	386 (431): 1.4–1.7
	R25/CTX	H404/Kv1.3	404 (449): 0.45–0.7
Gross and MacKinnon ^[5]			380 (425): 1.4–1.6
			425, 427, 428, 431, 448: more distant than 449, 438

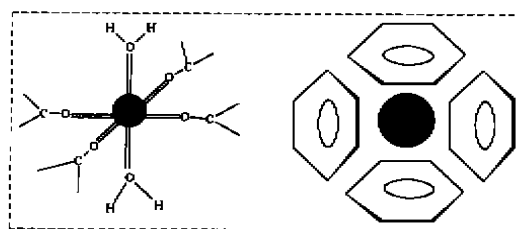
to dip into the membrane from the extracellular surface. These features defined the shape and dimension of outer mouth of channel, and formed the base of molecular modeling of K^+ channel (Fig 3, Plate 1, IA).

**Fig 2. Topography of residues in *Shaker* K^+ channel pore.**

The final structure (Fig 3, IB) was consistent with the characteristics derived from the experimental results. The 3 consecutive residues 447, 448, and 449 constituted the entrance of the pore. The narrowest region of the ion conduction pathway was formed by four Y445 residues, and the NH_2 -end residues in the P region formed the outer vestibule, which was large enough to accommodate scorpion toxins such as CTX and AgTx2.

Molecular mechanism for ion selectivity For several decades, the mechanism by which the K^+ channel protein selected K^+ for permeation had been a subject of speculation. There were two prevailing mechanisms suggested so far. One was oxygen cage mechanism, that was, the selectivity filter bound

potassium ion by encapsulating it, four electronegative oxygen ligands projecting into the transmembrane pore, fixed in a rigid geometry to mimic the waters of ionic hydration. The other was en face mechanism, in which the π electrons at the face of aromatic side chain might serve as the electronegative source for coordination to the potassium ions (Fig 4).

**Fig 4. Oxygen-cage mechanism and en face mechanism.**

According to our model, it seemed more likely that the two mechanisms worked in concert. At position 445, the ion selectivity was achieved through en face mechanism, while at position 447, it was carried out by means of oxygen cage mechanism (Fig 3, II). Given that was the case, the mutation results on these positions could be successfully explained and predicted. According to our proposed mechanism, mutation Y445F did not influence K^+ - π orbital interaction, and should have no effect on channel ion selectivity, which was consistent with experimental result^[13]. Though the ion selectivity at position 445 was destroyed after mutation Y445V, the resulting channel was still selective for K^+ over Na^+ , since another selectivity filter D447 remained intact^[15]. Likewise, it was

observed that mutation D378T (Kv2.1, corresponding to D447T in *Shaker*) markedly altered ion conduction, blockade, and the relative permeability of K^+ over Na^+ , but the ion selectivity order $K > Rb > Cs > Na$ remained unchanged^[14]. The reason for this was that Y445 retained channel ion selectivity. Compared with Y445, D447 was probably more critical for channel ion selectivity. It was clear that the concerted mechanism for ion selectivity worked quite well.

Interaction between scorpion toxins and channel The binding affinity and specificity of AgTx2 to the *Shaker* K^+ channel crucially depended on three residues R24, K27, and R31. By far the most important residue for AgTx2 affinity was K27, which was physically located on the central axis of the channel, with the α -amino group of this residue protruding slightly into the K^+ conduction pore in an extended conformation (Fig 3, III B). In contrast, K27 in CTX was somewhat off the central axis with its side chain curling (Fig 3, III A). As a result, this residue interacted with channel more weakly than that of AgTx2.

In addition to K27, the other two residues (R24 and R31) were positioned at two opposite ends of the AgTx2 along its pore long axis, interacting with the negatively charged D431 and aromatic residue F425, respectively. These two interacting pairs further enhanced the AgTx2 affinity to channel (Fig 3, III B). Similar interacting pairs (R25/D431, K31/D431), which favored CTX binding to channel, were also found in CTX-channel complex (Fig 3, III A). Compared with its functional counterpart R25 in CTX, the mobility of side-chain of R24 in AgTx2 was relatively restricted as a result of its interacting with the aromatic side-chain of F25. The low mobility was in favor of AgTx2 affinity.

A detailed inspection revealed that residues M29, R34, and Y36 in CTX (colored in blue) were all close to *Shaker* T449 in the bound complex (Fig 3, III A). Due to steric interaction, these residues were probably unfavorable to CTX blockade. CTX inhibited the *Shaker* K^+ channel 300-fold weaker than AgTx2, as could be easily explained and understood according to the binding differences discussed above. Therefore, the pore model

provided a structural basis for different affinity of AgTx2 and CTX to the pore entryway of the *Shaker* channel. In turn, these findings verified the soundness of our model.

Theoretical calculation of electrostatic potential It was clear that the inside of the pore was dominated by negative potential (Fig 3, IV A). When a K^+ ion passed through the pore, it should overcome a certain energy barrier resulting from its electrostatically attractive interaction with the pore. This electrostatic characteristic of the pore structure made it suitable for a cation channel.

After mutation D447T, we found that the electrostatic property at the entrance of the entryway and in the pore altered dramatically (Fig 3, IV B). The resultant channel ion selectivity, conductance, and toxin affinity would change greatly^[14]. More interestingly, the theoretical calculation results here also agreed well with molecular mechanism of channel ion selectivity, which was suggested in the above discussion.

The electrostatic property of the ion conduction pathway directly correlated with channel function. Given that the pore model proposed was valuable, it should be possible to qualitatively predict mutation results based upon the electrostatic potential change in the channel. Here, the electrostatic potential calculation results confirmed the creditability of our model.

Comments on the model According to the pore model here, the NH_2 -end residues in the pore region was relatively close to ion permeation pathway, directly correlating with channel ion selectivity. This structural feature coincided with Lipkind's model^[2]. Since our pore structure was built upon the latest results from SCAM and toxin studies, it was especially valuable for understanding the blocking mechanism of scorpion toxins.

The computer model presented here had three deficiencies. (1) It was composed of the bare pore region, through which the K^+ ion was believed to transverse the membrane. Any effect from the remaining amino acids which made up the complete K^+ channel was neglected. However, some residues from S4 - S5 linker and S6 segment attributed to ion selectivity as well^[15]. The pore model suggested here was not likely to be stable in

isolation. In actual *Shaker* K⁺ channel, it was possible that the pore structure was stabilized by the surrounding peptide. (2) The pore model here was static, and it was difficult to clarify channel dynamic behavior, such as the dynamic arrangement of the outer mouth during the C-type inactivation. (3) The structural restraints for modeling were derived mainly from the pharmacologically and electrophysiologically experimental results, some of which were probably questionable. Take the projection of a residue's side chain for example. When a residue was mutated to cysteine, we detected its orientation by thiol-labeling reagents. In general, the correct information could be derived, but it was not always the case. Once mutation resulted in great conformational change, we would probably draw an erroneous conclusion. Therefore, our pore structure was neither mature nor perfect, it required further improvements and validations. With the accumulation of the experimental data on voltage-gated K⁺ channels, more detailed and rational models were likely to be proposed.

Broadly speaking, the proposed structure was successful in explaining molecular mechanisms for channel function and many experimental results. It should be reasonable and useful for guiding further studies on potassium channels. More specifically, it might now be possible to design new agents that selectively block *Shaker* channel with the high affinity characteristic of toxin binding based upon our model.

REFERENCES

- Guy HR, Durell SR. Structural models of Na⁺ Ca²⁺ and K⁺ channels. In: Dawson DC, Frizzell RA, editors. Ion channels and genetic diseases. New York: Rockefeller Univ Press, 1995: 1-16.
- Lipkind GM, Hanck DA, Fozzard HA. A structure motif for the voltage-gated potassium channel pore. Proc Natl Acad Sci USA 1995; 92: 9215-9.
- Chandy G, Gutaman GA. Voltage-gated potassium channel genes. In: North RA, editors. Handbook of receptors and channels: ligand- and voltage-gated ion channels. Boca Raton, Florida: CRC Press, 1995: 1-70.
- Lü Q, Miller C. Silver as a probe of pore-forming residues in a potassium channel. Science 1995; 268: 304-7.
- Gross A, MacKinnon R. Agitoxin footprinting the *Shaker* potassium channel pore. Neuron 1996; 16: 399-406.
- Pascual JM, Shieh C-C, Kirsch GE, Brown AM. K⁺ pore

structure revealed by reporter cysteines at inner and outer surfaces. Neuron 1995; 14: 1055-63.

- Kürz LL, Zuhlke RD, Zhang H-J, Joho RH. Side-chain accessibilities in the pore of a K⁺ channel probed by sulfhydryl-specific reagents after cysteine-scanning mutagenesis. Biophys J 1995; 68: 900-5.
- Goldstein SAN, Pheasant DJ, Miller C. The charybdotoxin receptor of a *Shaker* K⁺ channel: peptide and channel residues mediating molecular recognition. Neuron 1994; 12: 1377-88.
- Aiyar J, Withka JM, Ruzzi JP, Singleton DH, Andrews GC, Lin W, et al. Topology of the pore-region of a K⁺ channel revealed by the NMR-derived structures of scorpion toxins. Neuron 1995; 15: 1169-81.
- Stocker M, Miller C. Electrostatic distance geometry in a K⁺ channel vestibule. Proc Natl Acad Sci USA 1994; 91: 9509-13.
- Naranjo D, Miller C. A strongly interacting pair of residues on the contact surface of charybdotoxin and a *Shaker* K⁺ channel. Neuron 1996; 16: 123-130.
- Hidalgo P, MacKinnon R. Revealing the architecture of a K⁺ channel pore through mutant cycles with a peptide inhibitor. Science 1995; 268: 307-10.
- Heginbotham L, Lu Z, Abramson T, MacKinnon R. Mutations in the K⁺ channel signature sequence. Biophys J 1994; 66: 1061-7.
- Kirsch GE, Pascual JP, Shieh C-C. Function role of a conserved aspartate in the external mouth of voltage-gated potassium channel. Biophys J 1995; 68: 1804-13.
- Lopez GA, Jan YN, Jan LY. Evidence that the S6 segment of the *Shaker* voltage-gated K⁺ channel comprises part of the pore. Nature 1994; 367: 179-82.

电压门控型钾通道孔区的分子建模

赵善荣, 陈凯先, 王蔚, 顾健德, 胡增建, 嵇汝运

(中国科学院上海药物研究所, 上海 200031, 中国)

关键词 分子模型; 钾通道; 蛋白质构象; 离子运输; 计算机辅助设计

目的: 建立和验证电压门控型钾通道的结构模型。
方法: (1)从实验和理论研究结果中提取结构约束条件; (2)建立满足这些约束条件的初始结构模型, 并进一步用限制性分子力学优化; (3)根据模型能否成功地解释通道功能分子机制和许多实验事实来判断其合理性。 **结果:** (1) 建立了一个孔区模型, 其中信号序列残基(对应 *Shaker* 439-446)以非周期性构象嵌入膜中并形成孔区比较窄的部分, 而孔区域的其它残基构成孔区外口; (2)

通道离子选择性在 445, 447 位置处分别通过阳离子- π 轨道作用机理和氧笼机理来实现; (3) CTX 和 AgTx2 与孔区的不同结合方式导致了它们通道

亲和力的差异; (4) 孔区内侧静电势主要为负。
结论: 构建的模型与从实验结果导出的限制信息是相一致的。

Kinetic properties of nicotinic receptors in cultured rat sympathetic neurons from superior cervical ganglia¹

ZHENG Jian-Quan, HE Xiang-Ping, YANG Ai-Zhen, LIU Chuan-Gui (*Institute of Pharmacology and Toxicology, Academy of Military Medical Sciences, Beijing 100850, China*)

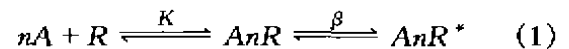
KEY WORDS nicotine; nicotinic receptors; sympathetic ganglia; pharmacokinetics; binding sites; patch-clamp techniques

AIM: To analyze the kinetic properties of the effect of nicotine on nicotinic acetylcholine receptors (nAChR) in the cultured sympathetic neurons from neonatal rat superior cervical ganglia (SCG).

METHODS: The whole-cell recording method of patch-clamp technique was used to record the currents induced by different concentrations of nicotine. The concentration-response of nicotine was fitted with Clark equation. **RESULTS:** Hill coefficient (1.097) was determined by fitting the nicotine responses of neuronal nAChR with Clark equation. The theoretical values of nicotine effect, calculated with Clark equation with $H = 1$, were basically identical with the practically recorded currents. **CONCLUSIONS:** Interaction of nicotine and nAChR in rat SCG fits a single binding site model.

Analyzing the kinetics of the effect of a drug on the target receptor is very important for elucidating its pharmacological properties and reactive mechanism. The first model to explain interacting process of a receptor and its ligand was put forward by Clark^[1], from which a sequential model to describe the concentration dependence of

acetylcholine (ACh) action was provided^[2,3].



In the sequential model 1, a receptor (R) can be activated by ACh (A) by forming an inactive ACh-receptor complex, where AnR and AnR* are inactive and active agonist-receptor complexes, respectively. And n is the number of ACh molecules activating a single receptor channel. According to the above scheme, the Clark equation could be transformed into the following equation:

$$E = E_{max} \cdot A^H / (K + A^H) \quad (2)$$

In the equation 2, E = response induced by nAChR agonist at a given concentration; E_{max} = the largest response of nAChR; A = agonists; K = equilibrium dissociation constant; H = Hill coefficient, just equating to n in the sequential model 1.

The sequential model is now widely used for the kinetic analysis of acetylcholine-receptor interaction of end-plate currents and single-channel currents of muscle nAChR^[4]. There are 2 ligand binding sites on the muscle nAChR and 2 molecules of agonist are required to excite a receptor molecule^[5,6] (ie $H = 2$). However, in the central nervous system, receptor binding assays have revealed a single class of binding sites in neuronal nAChR^[7-9]. Neuronal nAChR display a complicated diversity of the structure and biological functions compared with nAChR in skeletal muscles^[10]. It is still uncertain that whether 1 or 2 molecules of an agonist are required to activate 1 molecule of neuronal nAChR in sympathetic

¹ Project supported by the National Natural Science Foundation of China, No 39130090

Received 1996-06-25

Accepted 1997-03-15